Article

Study on Road Friction Database for Traffic Safety: Construction of Road Friction Measuring Device

Ichiro Kageyama [1,2], Yukiyo Kuriyagawa [2], Tetsunori Haraguchi [1,2,3], Tetsuya Kaneko [4], Minoru Nishio [5] and Atsushi Watanabe [2]

1 Consortium on Advanced Road-Friction Database, 1-4-31 Hachimandai, Sakura 285-0867, Japan; kageyama.ichiro@nihon-u.ac.jp (I.K.)
2 College of Industrial Technology, Nihon University, 1-2-1 Izumi-cho, Narashino 275-8575, Japan; kuriyagawa.yukiyo@nihon-u.ac.jp (Y.K.), watanabe.atsushi52@nihon-u.ac.jp (A.W.)
3 Institutes of Innovation for Future Society, Nagoya University, Furocho, Chikusaku, Nagoya 464-8603, Japan; haraguchi@nagoya-u.jp (T.H.)
4 Department of Mechanical Engineering for Transportation, Faculty of Engineering, Osaka Sangyo University, 3-1-1 Nakagaito, Daito 574-8530, Japan; kaneko@ge.osaka-sandai.ac.jp (T.K.)
5 Absolute Co., Ltd., 839-1 Kamikasuya, Isehara 259-1141, Japan; nis@absolute.gr.jp (M.N.)
* Correspondence: kageyama.ichiro@nihon-u.ac.jp (I.K.); haraguchi@nagoya-u.jp (T.H.)

Abstract: This paper deals with the possibility for construction of the database on friction coefficient on the actual roads from the viewpoint of traffic safety. A measurement algorithm is determined in order to construct road friction measuring device. Next, the tires used for measurement are selected and the characteristics are measured using bench tire characteristic tester, and the measuring device is designed and constructed based on the characteristics. Finally, using this device, the measurement results of the road friction characteristics for two types of road surfaces are shown.

Keywords: road friction; environmental information; measurement; friction estimation

1. Introduction

On actual roads, a road friction coefficient varies greatly depending on the pavement materials, state of road surfaces, tire structure and surface material, and so on. A systematic measurement method of the braking friction coefficient on an actual road and its creation in a database will be very important issues from the viewpoint of contribution to traffic safety and construction of a new driving support system including automated driving. Road friction characteristics, which are important for road safety [1], are treated differently by road-related engineers and automotive-related engineers. Among road-related researchers, the friction characteristic between the tire and the road surface is treated as a representative value of the friction characteristic at the time of locking, which is related to the dynamic friction coefficient. In particular, this value is important for road maintenance. On the other hand, among automotive-related researchers, the peak coefficient of friction is used as an important value in the study because of the maximum braking force. Especially in the vicinity of this characteristic, not only braking force but also lateral force is generated at the same time, which is a very important characteristic for vehicle safety. The friction characteristic at this time is the region where both static friction and dynamic friction generate force in the contact patch of the tire, so a force larger than the friction coefficient at the time of locking is generated. However, in the past it was difficult for drivers to maintain this area, so automotive engineers also used road friction at the time of locking as an index. It was found that when a system to prevent wheels from locking was introduced in railways, it not only suppressed uneven wear of wheels but also increased braking force, and it was introduced to landing tires in the aircraft field, and then spread to automobiles. By introducing this system, ABS, not only the braking distance could be shortened, but also the directional stability of the vehicle could be ensured. The

Preprints (www.preprints.org) | NOT PEER-REVIEWED | Posted: 2 August 2022 doi:10.20944/preprints202208.0033.v1

ABS system has become mandatory for ordinary vehicles in Japan these days, and braking distances close to the ideal on each road surface can be achieved when braking. For this reason, it is important to measure the characteristics of the force generated in the contact patch of the tire on various road surfaces and clarify these characteristics from the viewpoint of road safety. Figure 1 shows the results of μ-s characteristics measured using various tires under various road surface conditions. The lateral axis of Figure 1 represents the coefficient of friction, and the longitudinal axis represents the slip ratio. The slip ratio is defined by Equation (1).

$$s = \frac{v - \omega r}{v} \tag{1}$$

where s: slip ratio; ω: angular velocity of tire; r: tire radius; and v: vehicle speed.

From Figure 1, it can be seen that the peak friction coefficient (hereinafter referred to as peak μ) mainly occurs at a slip ratio of 0.2 or less. Further, the value of the slip ratio 1 becomes the value of the friction coefficient at the time of locking (similarly, the locking μ). Further, the peak μ shows a value of about 1.2 times or more than that of the lock μ. In addition, the peak μ value fluctuates greatly depending on the road surface conditions such as dry and wet surfaces and the difference in tires, so there is a problem that the braking distance of the vehicles will differ by about twice even under normal road surface conditions. Furthermore, it is known that the braking distance on snow and ice roads differs by about 10 times the braking distance on dry surfaces. Therefore, from the viewpoint of vehicle safety, it is very important to know these characteristics in front of the vehicles. In particular, in autopilot vehicles, which are expected to become widespread in recent years, the controller needs to perform these safety management, and especially in systems of level 4 or higher where the responsibility of the vehicle is important, this information is indispensable. For this reason, it is necessary to introduce a forward road friction estimation system, but at present there is no such road friction database, which is a bottleneck in the construction of such a system.

From this point of view, this study examines the construction of a measurement method for constructing the database on ordinary roads.

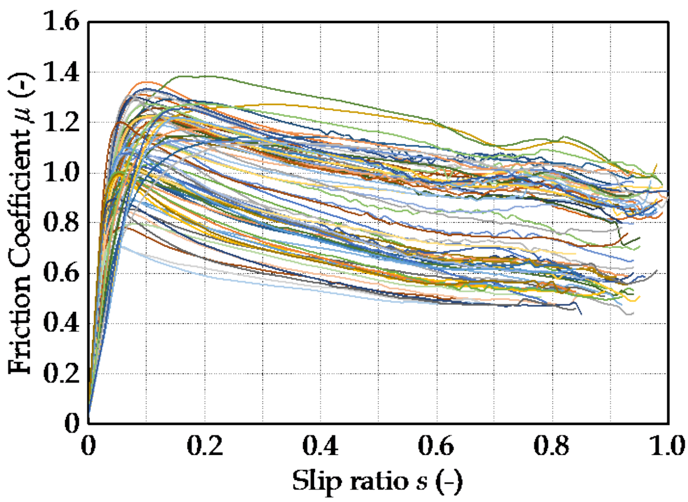

Figure 1. Characteristics of the road friction coefficient.

2. An estimation method for Road friction coefficient

2.1. Identification algorithm

Since the road friction characteristics vary depending on the road position, it is necessary to develop a method for continuously measuring the friction characteristics of or-

Preprints (www.preprints.org) | NOT PEER-REVIEWED | Posted: 2 August 2022 doi:10.20944/preprints202208.0033.v1

dinary roads. Normally, devices that measure μ-s characteristics have used tire characteristic testers mounted on trailers or buses to gradually apply braking while driving and to grasp the braking force characteristics. However, such a method requires the assumption that the characteristics of the measured road surface are constant during sensing, but the ordinary road surface conditions may change, and it is necessary to continuously measure these μ-s characteristics. Therefore, in the past, our group has proposed a μ-s characteristic estimation method using the simple magic formula as Equation (2), which was proposed by Prof. Pacejka of Delft University of Technology [2].

$$\mu = a\sin\{b\tan^{-1}(cs)\} \tag{2}$$

Here, the μ-s characteristics can be identified by determining the coefficients a, b and c in Equation (2) using the experimental data. Figure 2 shows an example of identification using this method. In Figure 2, the slip ratio is shown as a percentage, and the data used are those of s=3%, 10% and 17% data, marked with yellow circles in Figure 2. The result of MF identification using these three points is shown by the red line. The experimental results at this time are described by blue lines, and the identification results express the characteristics well.

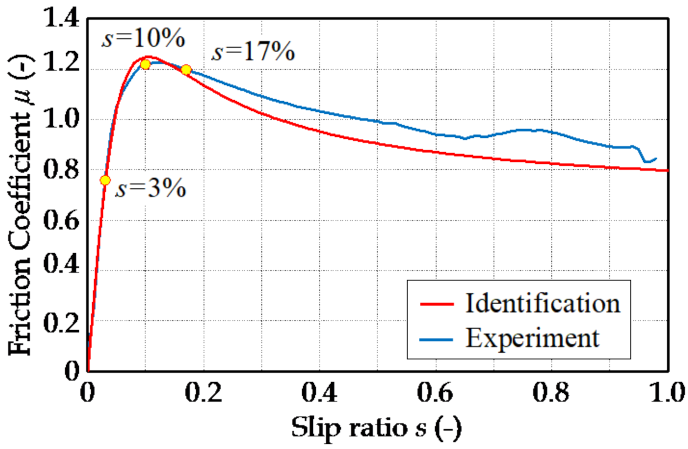

Figure 2. An example of estimated result using MF.

2.2. Verification of the algorithm

Using the experimental results shown in Figure 1, the result of identification is confirmed assuming that three points of data have been obtained. Equation (3) is obtained by differentiating the MF with respect to s.

$$\frac{d\mu}{ds} = \frac{abc\cos\{b\tan^{-1}(cs)\}}{c^2s^2+1} \tag{3}$$

Since the value of Equation (3) equals to 0 represents the peak μ, the slip ratio s_P that generates the peak μ can be obtained as in Equation (4).

$$s_P = \frac{\tan\left(\frac{\pi}{2b}\right)}{c} \tag{4}$$

Substituting this s_P into MF shown in Equation (2), the peak μ is given by Equation (5).

$$\mu_{max} = a\sin\left[b\tan^{-1}\left\{\tan\left(\frac{\pi}{2b}\right)\right\}\right] \tag{5}$$

Another important factor that can be obtained from the μ-s characteristics is the standardized braking stiffness K_B. This means a tangential value of s=0 of the μ-s characteristics, and the value obtained by multiplying this value by the tire load is the braking stiffness. Therefore, by substituting s=0 into Equation (3), the standardized braking stiffness can be obtained by Equation (6).

$$K_B = \frac{\partial \mu(s)}{\partial s}|_{s=0} = abc \tag{6}$$

These identification results are confirmed using the experimental results shown in Figure 1. Therefore, Figure 3 shows a comparison between the experimental results and the identification results of the peak μ shown in the Equation (5) and the K_B shown in the Equation (6). From these results, the peak μ has a correlation coefficient of 0.982 and the K_B has a correlation coefficient of 0.949 and is sufficiently estimated.

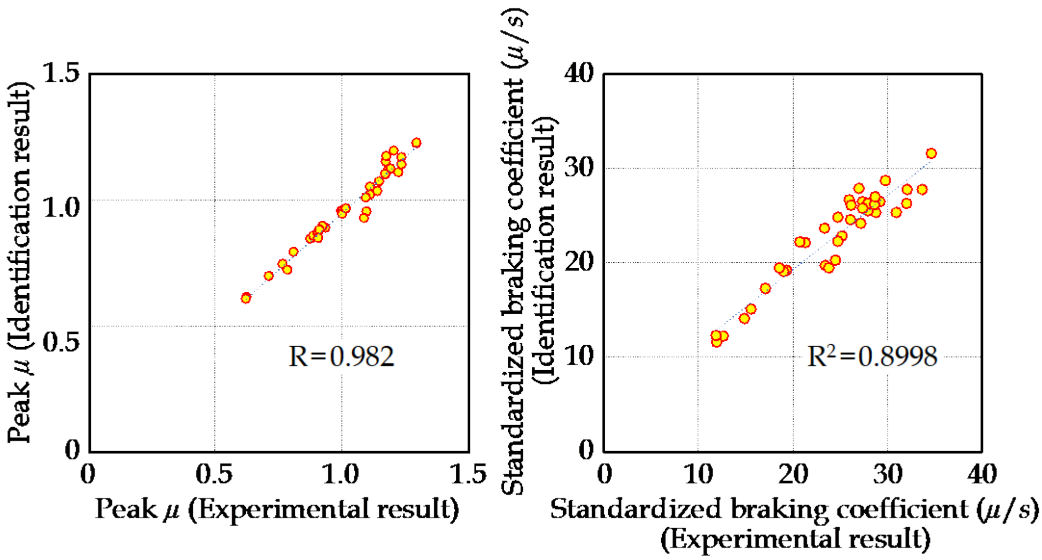

(**a**) Peak μ (**b**) μ/s

Figure 3. Comparison between experimental results and identification results.

Next, the value of lock μ, which is emphasized by road engineers, is compared. In the analysis, the estimation result can be obtained by substituting s=1 for the MF in Equation (2). In this study, as shown in Figure 2, because of identification at three set data in the region near the peak μ, it is expected that the estimation accuracy of the lock μ will deteriorate. Therefore, Figure 4 shows a comparison between the experimental results and the identification results of lock μ.

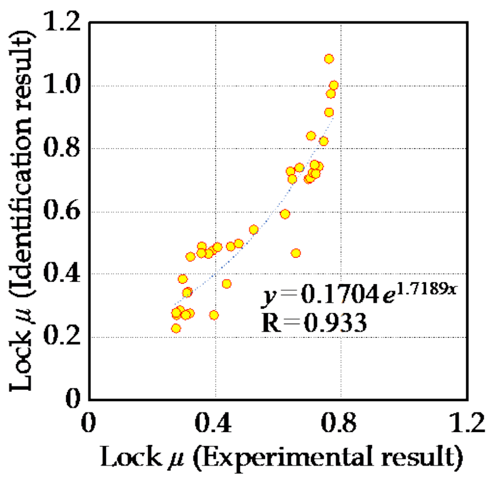

Figure 4. Comparison between experimental results and identification results at lock μ.

From Figure 4, the lock μ obtained from the experiment and the lock μ obtained by using the MF have strong non-linearity, and the value by the MF is smaller in the low μ region. Therefore, when getting the μ-s characteristics widely, it is preferable to include an estimated value of lock μ for identification. From experience so far, peak μ in these low

Preprints (www.preprints.org) | NOT PEER-REVIEWED | Posted: 2 August 2022 doi:10.20944/preprints202208.0033.v1

μ regions occurs at relatively low slip ratios. Experience has shown that the reduction in lock μ is relatively large relative to the peak μ that occurs at such low slip ratios. Therefore, we added data on wet roads where peak μ appears in a region with a low slip ratio, focused on the relationship between the slip ratio and the ratio of lock μ by peak μ, and the results are shown in Figure 5. A logarithmic approximation of this relationship is shown in Figure 5, but since these correlation coefficients are relatively high at about 0.81, the peak μ obtained from the analysis of MF using the three-set data obtained from the experiment is used to estimate for lock μ [3]. Use the resulting lock μ to reidentify the MF and obtain a modified μ-s diagram. Using the method shown here, we will finally adopt the method of grasping the modified μ-s characteristics from the three sets of data obtained from the experiment.

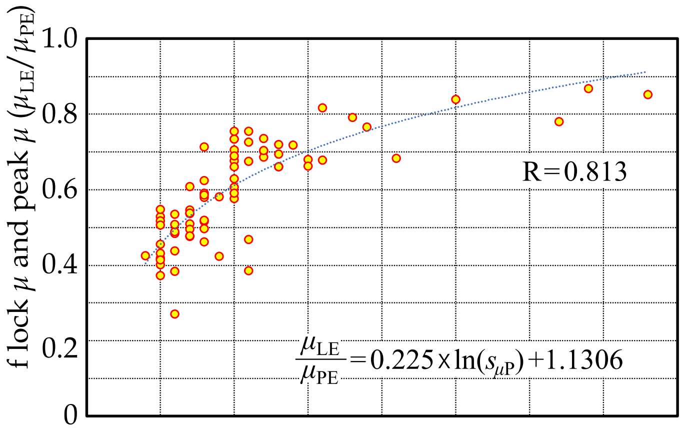

Figure 5. Relationship between the slip ratio and the ratio of lock μ by peak μ.

3. Fundamental design of Measurement trailer system

3.1. Overview of measurement system

To measure the three sets of slip ratio and the road friction coefficient at the same time, measurement trailer is designed as shown in Figure 6. Two-axis load cells are placed on each measurement tire, and the angular velocity of each tire is measured by a disk that generates 24 pulses per rotation. The measurement system adopts the structure shown in References [4,5,6]. As shown in Figure 6, the basic structure uses sprockets with different numbers of teeth to continually reproduce the braking state of the measuring tire. As a result, the measured tire can be run at a constant slip ratio, and the main tire runs on the drive side (slip ratio negative) with respect to the vehicle speed, and the measured tire runs on the braking side (slip ratio positive) with a substantially constant slip ratio. At the same time, braking force, vertical load and wheel speed are measured by a load cell and pulse sensor mounted on the axle of the measuring wheel. By preparing three sets of the relationship between the slip ratio and road friction coefficient, the system can obtain the required reference measurement data. In consideration of trailer stability at highways and trailer size, two measurement tires are placed in front of the trailer tires, and one tire is placed in the rear. Therefore, the rough design is shown in Figure 7.

Preprints (www.preprints.org) | NOT PEER-REVIEWED | Posted: 2 August 2022 doi:10.20944/preprints202208.0033.v1

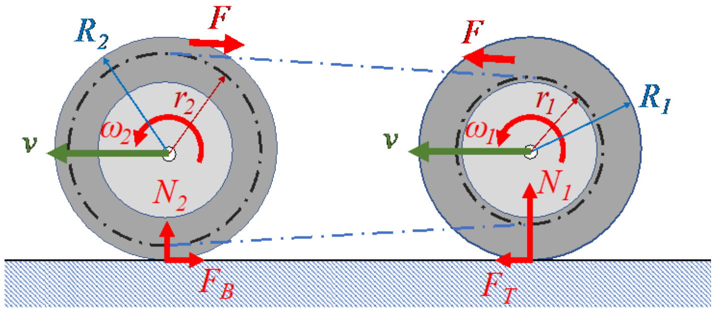

Figure 6. Mechanical properties between two tires [4,5].

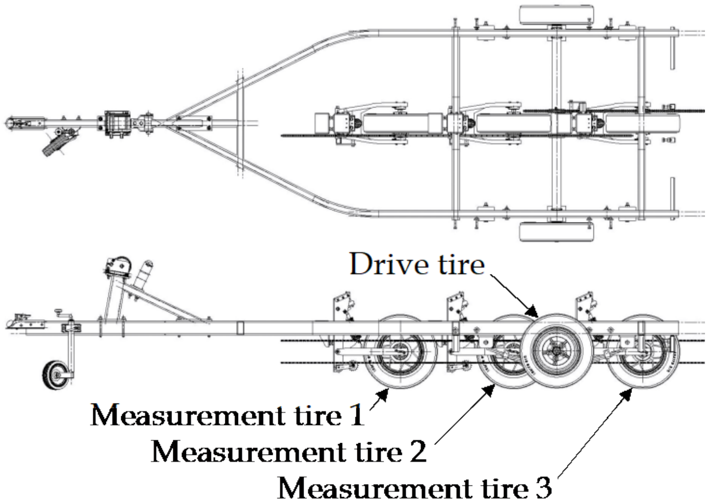

Figure 7. Fundamental design for trailer [6].

Here, what kind of tire is used as measurement tires and how to set the load and inner pressure of the tires are important. Especially for measurement for ordinary road in Japan, it is necessary to design according to the standard of trailer pulled by passenger car, and it is necessary to keep the total weight less than 750kgf. Within these conditions, it is necessary to determine the measurement tires. to adopt a narrow and small diameter measuring tire.

3.2. Determine of measurement tire

Since there are a total of five tires on trailer tires and on measurement tires, and the weight of the entire trailer is determined, it is not possible to take a large load per each measurement tire. Further, in general, the friction coefficient of rubber depends on the surface pressure, and the smaller this value is, the larger the friction coefficient is. In order that the μ-s characteristics measured by this system and the characteristics of tires installed on general vehicles do not differ significantly, in determining the measurement tire, therefore, it is necessary to introduce a tire with a small diameter, narrow width, and a small standard set load. Finally, we adopt 125R12-62S that satisfies these situations, including the possibility of supplying measurement tires in the future.

3.3. Determination of tire setting conditions

Since the tire has been determined, it is necessary to determine the load and internal pressure as factors that change the tire characteristics. An appropriate measurement condition is determined using the tire characteristic tester shown in Figure 8. The measured road surface uses Safety Walk ™, which is a pseudo-paved surface, and has a slightly higher friction coefficient than ordinary asphalt pavements.

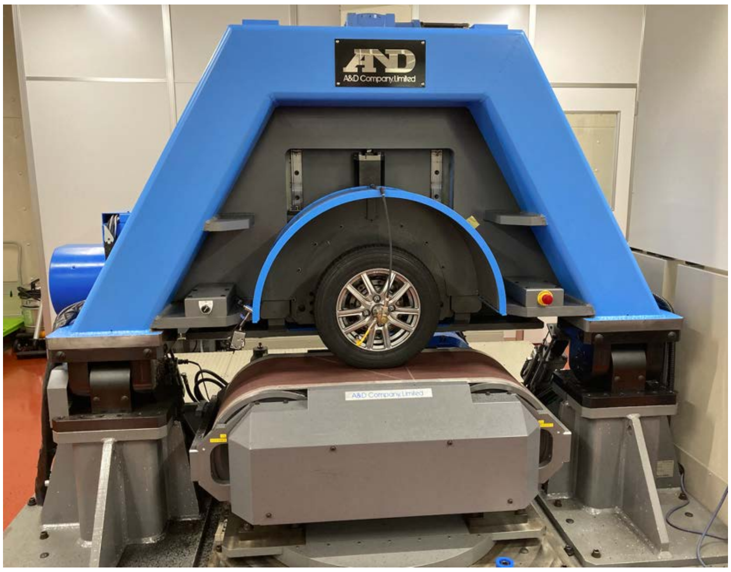

Figure 8. Tire characteristic tester with measurement tire.

Considering the load that can be set on the measurement trailer, we determine to set the load conditions to 5 levels (250, 500, 750, 1000, 2000N). Also, considering the internal pressure of the tire, set it in 4 levels (150, 200, 250, 300 kPa) and measure by combining these. As an example, Figure 9 shows the results of the friction coefficient when the load changes at an internal pressure of 200 kPa. From Figure 9, by reducing the load, the value of the peak μ increases and the value of the slip ratio that generates the peak μ increases. To clarify these relationships, Figure 10 shows the relationship between the change in peak μ with respect to the load and the slip ratio that generates the peak μ with respect to the load. It is necessary to determine the tire load in consideration of these characteristics, but the load is determined to be 500N in consideration of the total load of the trailer. Focusing on the peak μ in Figure 9, it shows a larger value than the peak μ of ordinary tires. Therefore, it is necessary to bring this value closer to that of ordinary tires due to changes in internal pressure.

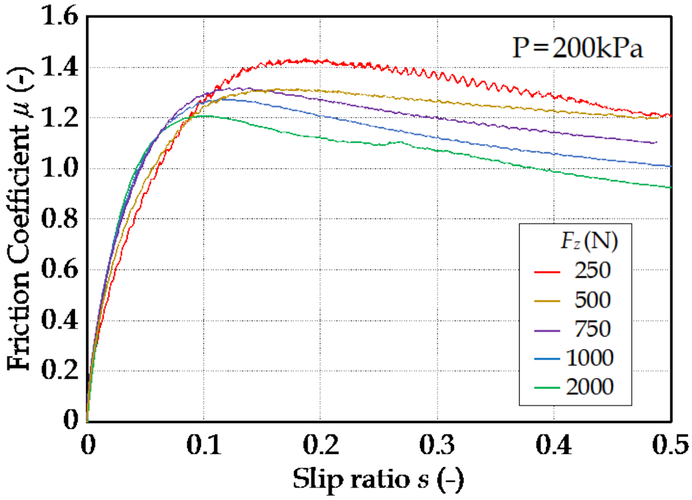

Figure 9. μ-s characteristics against load changes.

Preprints (www.preprints.org) | NOT PEER-REVIEWED | Posted: 2 August 2022 doi:10.20944/preprints202208.0033.v1

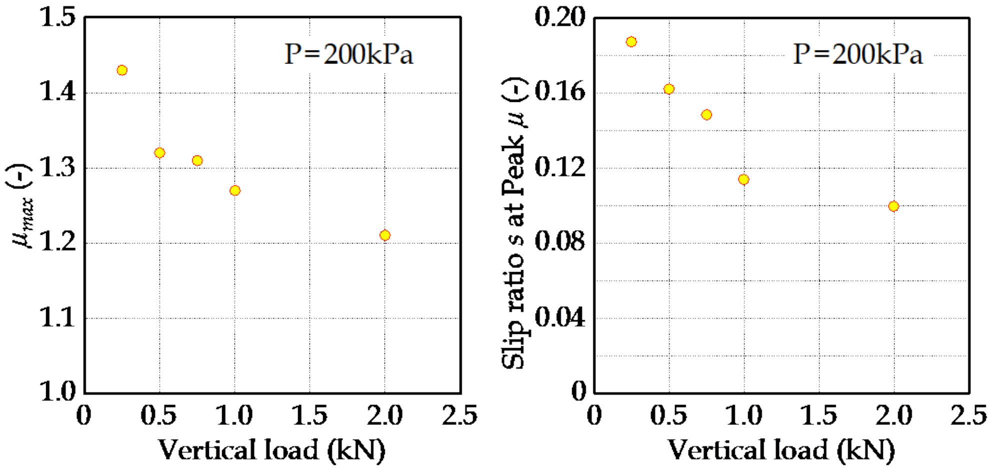

(**a**) μ_{max} (**b**) Slip ratio s

Figure 10. Characteristics of measurement tires against load changes.

Next, Figure 11 shows the change in μ-s characteristics with respect to the change in internal pressure when the tire load is 500 N. From Figure 11, the μ-s characteristic change in the internal pressure change is not as large as the characteristic change in the load change, but the peak μ value increases as the internal pressure increases. Therefore, the change in peak μ with respect to the change in internal pressure and the value of the slip ratio at that time are shown in Figure 12. From Figure 12, as the internal pressure decreases, the value of the peak μ decreases, approaching the characteristics of ordinary tires. However, if the internal pressure is too low, it will lead to uneven wear and heat generation on the tread surface, so it is necessary to suppress it to the ordinary usage conditions of the tire. As a result of these studies, it is decided that internal pressure 150 kPa at the load 500N is acceptable, and this is set as the setting condition at the experiment.

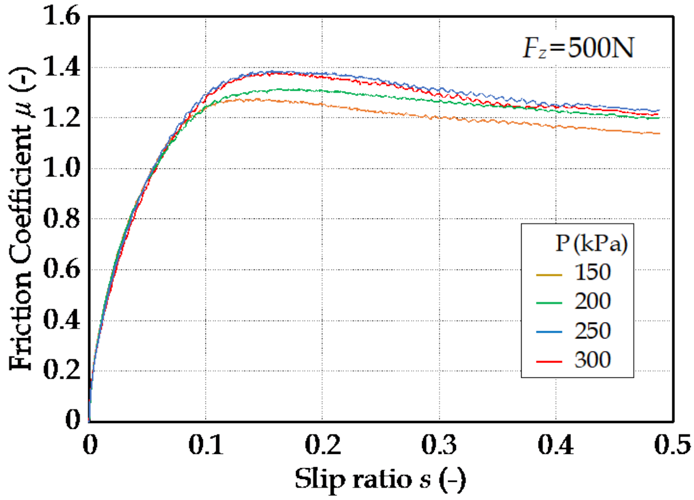

Figure 11. μ-s characteristics against internal pressure changes.

 doi:10.20944/preprints202208.0033.v1

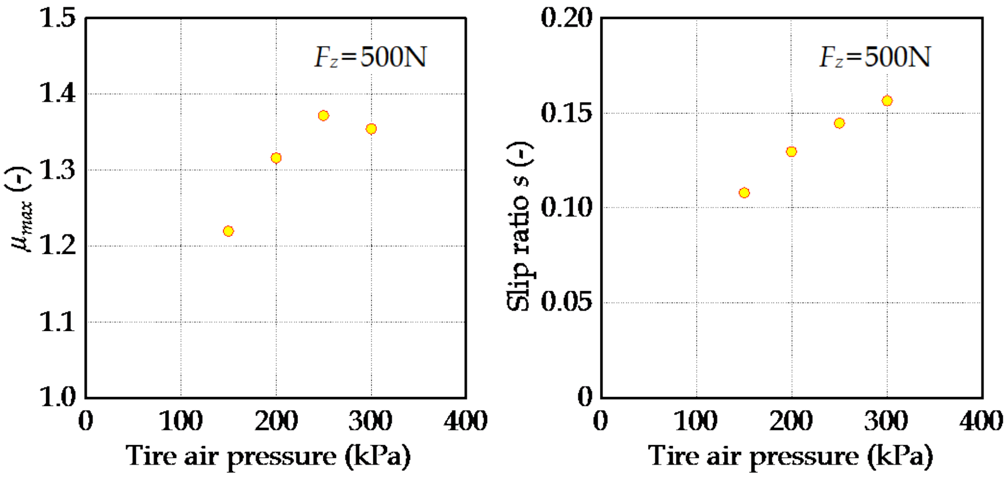

(**a**) μ_{max} (**b**) Slip ratio s

Figure 12. Characteristics of measurement tires against internal pressure changes.

4. Experiment of Road friction measurement

4.1. Constructed trailer system

A trailer for measurement was constructed using the tire conditions determined in the previous section. The entire view of the constructed trailer is shown in Figure 13, and the circumference of the measurement tire is shown in Figure 14. As shown in Figure 14, the axes of each measurement tire are arranged with two load cells on the left and right sides, and the braking force and the load are calculated using these output results and further considering the chain tension. Figure 15 shows the force relationship generated on the first wheel (measurement tire at the front position). In Figure 15, the balance of force and moment in each axial direction is given by Equations (7)-(10).

Figure 13. Constructed measurement trailer system.

Preprints (www.preprints.org) | NOT PEER-REVIEWED | Posted: 2 August 2022 doi:10.20944/preprints202208.0033.v1

Figure 14. Circumference of the measurement tire.

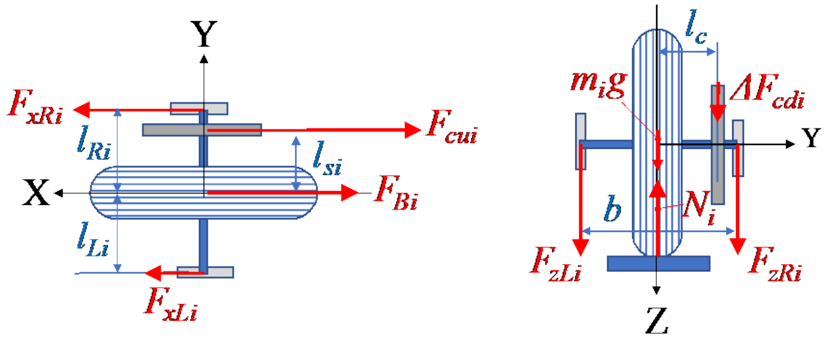

(**a**) Top view (**b**) Back view

Figure 15. Forces relationship generated on the *i*-th tire (Subscript '*i*' is the tire number).

For the X-axis forces:

$$F_{xLi} + F_{xRi} = F_{Bi} + (F_{cui} + F_{cdi}) \cos \Delta\theta_i \tag{7}$$

Here, $\Delta\theta_i$ indicates the angle of the chain tension from the horizontal. The symbols of each force in the formula are shown in Figure 15, and the suffix means the tire number. For the *Z* axis forces:

$$F_{zLi} + F_{zRi} + (F_{cui} - F_{cdi}) \sin \Delta\theta_i + m_i g = N_i \tag{8}$$

For the moment around the *X* axis:

$$-l_{Li}F_{zLi} + l_{Ri}F_{zRi} + l_{si}(F_{cui} - F_{cdi}) \sin \Delta\theta_i = 0 \tag{9}$$

For the moment around the *Z* axis:

$$(l_{Li}F_{xLi} - l_{Ri}F_{xRi}) + l_c(F_{cui} + F_{cdi}) \cos \Delta\theta_i = 0 \tag{10}$$

Using Equations (7)-(10), the braking force and the reaction force are derived as Equations (11) and (12).
The braking force:

$$F_{Bi} = F_{xLi} + F_{xRi} + \frac{l_{Li}F_{xLi} - l_{Ri}F_{xRi}}{l_{si}} = \left(1 + \frac{l_{Li}}{l_{si}}\right) F_{xLi} + \left(1 - \frac{l_{Ri}}{l_{si}}\right) F_{xRi} \tag{11}$$

The reaction force:

$$N_i = \left(1 + \frac{l_{Li}}{l_{si}}\right) F_{zLi} + \left(1 - \frac{l_{Ri}}{l_{si}}\right) F_{zRi} + m_i g \tag{12}$$

Here, $m_i g$ in the formula is the weight from the load cell to the contact point. Therefore, the friction coefficient is given by Equation (13) from the Equations (11) and (12).

Preprints (www.preprints.org) | NOT PEER-REVIEWED | Posted: 2 August 2022 doi:10.20944/preprints202208.0033.v1

$$\mu_i = \frac{F_{Bi}}{N_i} \tag{13}$$

Although the chain mounting position and the chain tension direction are different between the second tire and the third tire, the coefficient of friction of each tire can be obtained in the same process.

The slip ratio of each tire is obtained from the relationship between the free rolling distance of the tire and the rolling distance when the chain was attached, and as a result, the following relationship was obtained.

Slip ratio of measurement tire 1: 0.954%

Slip ratio of measurement tire 2: 7.057%

Slip ratio of measurement tire 3: 17.23%

Slip ratio of trailer tire: -2.62%

The trailer tire has a negative slip ratio (driving state) because it is driven by the other measurement tires.

4.2. Measurement of road friction

In this paper, we tried to measure two types of pavements ("Fine particle asphalt mixture" and "Coarse particle asphalt mixture") as shown in Figure 16.

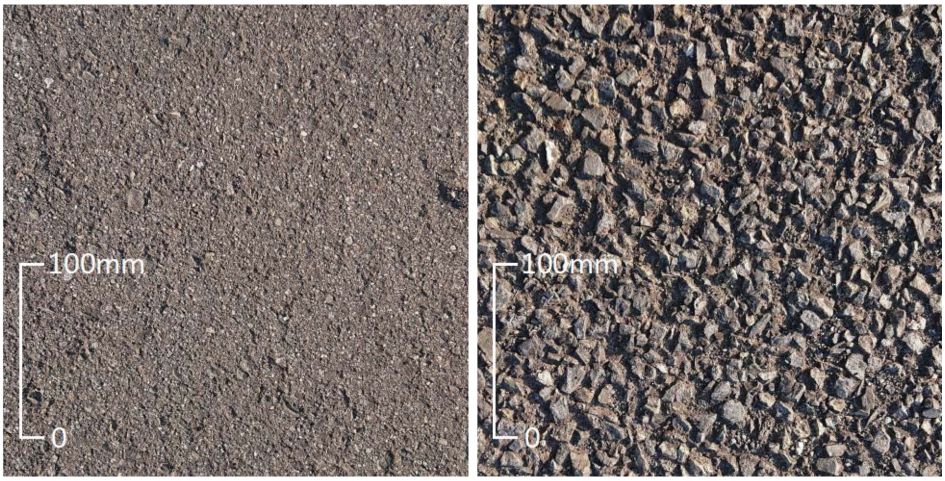

(**a**) Fine particle asphalt mixture (Asphalt pavement) (**b**) Coarse particle asphalt mixture (Permeable pavement)

Figure 16. Pavement surface used for measurement.

Next, the measurement results and identification results on each road surface are shown. First, the result of fine particle asphalt mixture is shown in Figure 17. Three points are the measurement results, and the blue line is the result of identification by the MF using these three points. Next, using the peak μ of this blue line and the slip ratio at that time, the lock μ is obtained by the estimation method shown in Figure 17, and the identification result including this point is shown by the red line. The coefficients a, b, and c of the MF are shown in Figure 17, suffix '0' is the identification result using the first three points, and '*' indicates the final identification result.

Preprints (www.preprints.org) | NOT PEER-REVIEWED | Posted: 2 August 2022 doi:10.20944/preprints202208.0033.v1

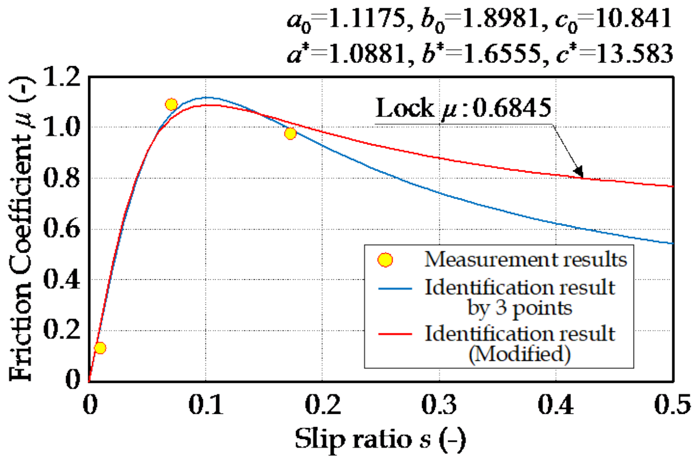

Figure 17. The result of the 'fine particle asphalt mixture'.

Similarly, the results for coarse particle asphalt mixture are shown in Figure 18. In Figure 18 as well, the same analysis as in Figure 17 is performed. From Figures 17 and 18, the change in μ-s characteristics due to the difference surface of the road is clearly represented.

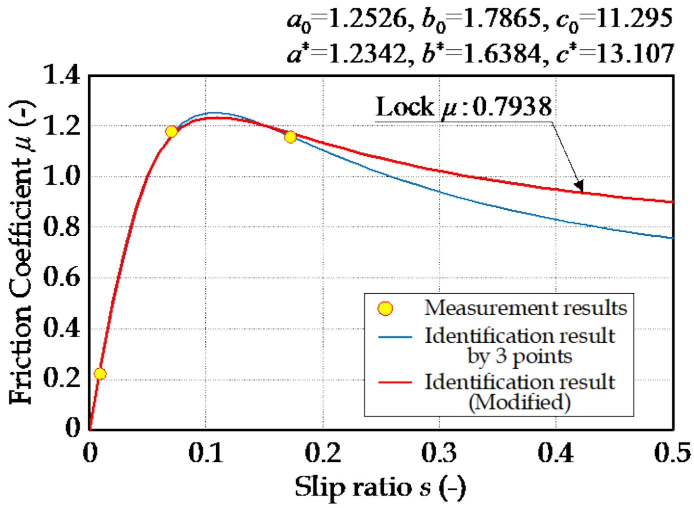

Figure 18. The result of the 'coarse particle asphalt mixture'.

Next, it is necessary to compare these differences with the tire characteristics measured by the bench tester and confirm the validity of the results measured by this device. These results are shown in Figure 19 to confirm the characteristic difference due to the difference in the road surface for the same tires and the same setting conditions. These need to be considered separately in three regions. The first is the characteristic of rising with strong linearity, which is the region for confirming the above-mentioned K_B.

The next is the region where the peak μ value and its slip ratio value appear. The last is the region where the characteristic decline appears after the peak μ passed. The first region is that depends on the shearing force characteristics of the tire tread rubber, and if the tire setting conditions are the same, the μ-s characteristics have relatively the same inclination. From Figure 19, this inclination has an almost constant value under three conditions such as a bench test result and difference in the pavement surfaces. The conclusions in this region can be seen as generally reasonable results. In the second region, the peak μ value and the situation to reach it are important evaluation criteria. The transition from the relatively linear inclination region to the peak μ involves the transition from the adherence region to the sliding region in the contact patch of the tire. Therefore, when the tire setting conditions are the same, generally, the peak μ is reduced due to the decrease in the road surface friction coefficient and appears in a region where the slip ratio at which the peak μ is generated is low. From the results of this experiment, the change in the characteristics can be clearly seen, and the results in this area are evaluated to be reasonable.

Focusing on the characteristics after passing the peak μ, which is the last region, the characteristics on the actual road show relatively the same characteristics, whereas the bench test results show that the decrease in this region is relatively small. This bench tester uses a belt-type road surface, and a pseudo paved road surface is attached to the surface. It is known that this surface has relatively high shear characteristics of individual irregularities from the viewpoint of maintaining the durability of the test road surface. For this reason, the state maintenance performance of the adherence region in the ground plane is improved, and it is considered that the transition to the sliding region appears relatively late. Considering these, it can be evaluated that the characteristics of this region are reasonable.

Considering the examination divided into these three areas, it is judged that the value measured by this device is appropriate.

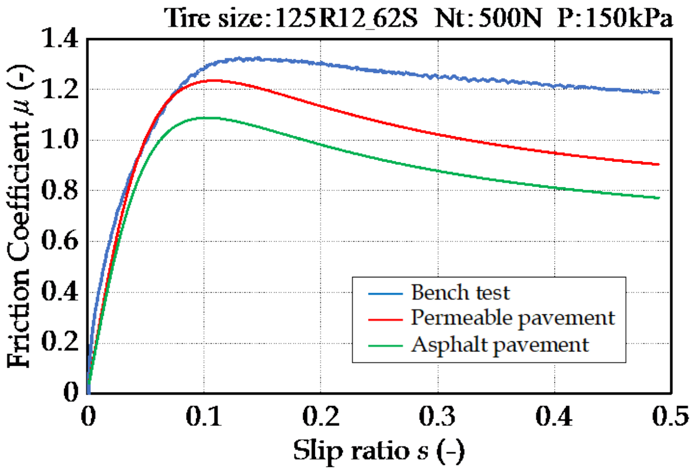

Figure 19. Comparison between bench test result and experimental results using MF.

5. Conclusions

In this study, to ensure the road traffic safety of ‘Advanced driver assist system’ and ‘Automated driving system’, which are expected to become widespread in the future, we examined the possibility of constructing a road friction characteristic measurement system for the purpose of providing road friction information. As a result, we came to the following conclusions.

(1) Characteristic measurements were performed on two types of road surfaces (‘Fine particle asphalt mixture’ and ‘Coarse particle asphalt mixture’), and identification using the MF and characteristic modified method using lock μ estimation were shown.

(2) By examining and comparing the results of the friction characteristics of the two types of actual road surfaces and the results of the bench test in three areas, it was confirmed that the original purpose could be achieved.

(3) As a result, it can be seen that a new road surface friction characteristic measurement system based on the μ-s characteristics has been constructed.

As future tasks, it is necessary to study the measurement of characteristics on various ordinary road surfaces include dry and wet roads, snowy and icy roads, and the creation of a database of them. Furthermore, it is necessary to conduct research toward the construction of a forward road friction estimation system by constructing a database of road surfaces under various conditions and at the same time adding a database of environmental changes.

 doi:10.20944/preprints202208.0033.v1

Author Contributions: Conceptualization, T.H. and I.K.; Data curation, I.K. and A.W.; Formal analysis, I.K. and Y.K.; Funding acquisition, T.H. and I.K.; Investigation, T.H., T.K. and M.N.; Methodology, I.K. and Y.K.; Project administration, T.H.; Resources, T.K. and M.N.; Validation, Y.K. and A.W.; Writing— original draft, I.K.; Writing—review & editing, T.H. All authors have read and agreed to the published version of the manuscript.

Funding: This research received no external funding.

Institutional Review Board Statement: Not applicable.

Informed Consent Statement: Not applicable.

Acknowledgments: A part of this research was supported by NEXCO East Japan research grant in Japan, and we would like to express our gratitude to all concerned.

Conflicts of Interest: The authors declare no conflict of interest.

References

1. Ando et.al. Dynamic friction on road surface and road surface management level and slip accident (in Japanese). *Civil engineering Journal* **2010**, *52*, 56-59.
2. Pacejka, H. B.; Bakker, E. The magic formula tire model. *Supplement to Vehicle System Dynamics* **1992**, *21*, 1-18.
3. Kuriyagawa, Y.; Kageyama, I.; Haraguchi, T.; Kaneko, T.; Asai, M.; Tahira, S.; Matsumoto, G. Study on Measurement for Friction Characteristics on Actual Road Surface: Construction of estimation method for road friction characteristic indexes (in Japanese). *Trans. JSAE* **2022**, *53*, 379-384.
4. Kageyama, I.; Kobayashi, Y.; Haraguchi, T.; Asai, M.; Matsumoto, G. Study on Measurement for Friction Characteristics on Actual Road Surface (in Japanese). *Trans. JSAE* **2020**, *51*, 924-930.
5. Kageyama, I. Kuriyagawa, Y.; Haraguchi, T.; Kaneko, T.; Asai, M.; Matsumoto, G. Study on the Road Friction Database for Automated Driving: Fundamental Consideration of the Measuring Device for the Road Friction Database. *Appl. Sci.* 2021, *12*.
6. Kageyama, I. Kuriyagawa, Y.; Haraguchi, T.; Kaneko, T.; Nishio, M.; Matsumoto, G. Construction of Characteristic Measurement System for Ordinary Road Friction (in Japanese). *Proceedings of JSAE annual meeting* **2022**, No.20225321.